

# Cp<sub>2</sub>TiCl-Catalyzed Epoxide Radical Ring Opening: A New Initiating Methodology for Graft Copolymer Synthesis

Alexandru D. Asandei<sup>\*,†,‡</sup> and Gobinda Saha<sup>†</sup>

*Institute of Materials Science, Polymer Program, and Department of Chemistry, University of Connecticut, 97 North Eagleville Rd., Storrs, Connecticut 06269-3136*

*Received August 15, 2006; Revised Manuscript Received October 16, 2006*

**ABSTRACT:** The first example of the use of epoxides in radical grafting copolymerizations was exemplified by the grafting of poly(methyl methacrylate) (PMMA), poly(butyl methacrylate) (PBMA), poly(butyl acrylate) (PBA), and poly(styrene) (PSt) from poly(glycidyl methacrylate) (PGMA) and from copolymers of GMA with MMA and St as well as by the iterative synthesis of mixed arm graft copolymers such as (PGMA-*g*-PMMA)-*g*-PSt and ((PGMA-*g*-PMMA)-*g*-PSt)-*g*-PBMA with a wide range of molecular weights and compositions. The grafting was demonstrated by a combination of gel permeation chromatography (GPC), NMR, and differential scanning calorimetry (DSC) investigations. The polymerization is initiated by the Cp<sub>2</sub>TiCl-catalyzed radical ring opening of the epoxide group of GMA and is optionally controlled by CuBr<sub>2</sub>/bipyridyl. This methodology does not require any epoxide protection/deprotection steps and provides the typical advantages of radical polymerizations and convenient access to complex macromolecular architectures.

## Introduction

Graft copolymers contain side-chain branches emanating from different points along the polymer backbone.<sup>1</sup> Variations in the nature of the main chain and side chains and in the length and polydispersity of the backbone and branches as well as in graft density<sup>2</sup> determine the properties and the associated complexity of the synthetic effort. Well-defined graft copolymers can be prepared by the “onto”, “through”, and “from” major grafting protocols. In the “grafting onto” process, end-functionalized polymer chains are attached to the main chain of another polymer via coupling reactions with functional groups along its backbone.<sup>3</sup> However, difficulties associated with the poor control over the quantitative coupling have confined the “grafting onto” method to a narrow range of applications. The “grafting through” approach is based on the synthesis of a well-defined macromonomer, followed by its copolymerization with a low molecular weight comonomer.<sup>4</sup> Although control over length and polydispersity can be achieved for both backbone and side chains, the grafting density is controlled by the reactivity ratios. The “grafting from” process is based on the synthesis of a macroinitiator containing suitable initiating groups along the backbone.<sup>5</sup> The high initiator efficiency, the ability to manipulate initiator distribution along the main chain, and the side chain length control afforded by living polymerization techniques make the “grafting from” process the preferred option in the synthesis of well-defined graft copolymers. The ability of living radical polymerization (LRP) to control molecular weight and polydispersity and its multiple advantages over ionic living polymerizations have enabled it to become one of the most efficient and robust synthetic methods in modern polymer chemistry. The molecular weight ( $M_n$ ) and polydispersity ( $M_w/M_n$ ) control in LRP is afforded by the reversible termination of growing chains with persistent radicals<sup>6</sup> or degenerative transfer (DT) agents<sup>7</sup> and proceeds mechanistically via either atom transfer (ATRP),<sup>7,8,14</sup> dissociation–combination (DC),<sup>9,10</sup> or

degenerative transfer (DT)<sup>7,11–13</sup> processes. The wide applications of LRP in the synthesis of complex, well-defined macromolecular structures<sup>14–16</sup> including block, graft, hyperbranched, and multiarm stars copolymers have also stimulated extensive efforts in the development of novel initiators and catalytic systems.

Currently, in addition to applications in  $\alpha$ -olefin coordination polymerizations<sup>17</sup> and organometallic reactions,<sup>18</sup> there is increased interest in the radical organic chemistry of early transition metals.<sup>19</sup> One of the most successful examples, the paramagnetic Cp<sub>2</sub>Ti(III)Cl<sup>20</sup> complex, is inexpensively available from the reduction of Cp<sub>2</sub>Ti(IV)Cl<sub>2</sub> with Zn.<sup>21</sup> Cp<sub>2</sub>TiCl is a very mild one-electron-transfer agent which catalyzes a variety of radical reactions,<sup>22</sup> including the radical ring opening (RRO) of epoxides<sup>23</sup> and the single electron transfer (SET)<sup>24</sup> reduction of carbonyls and their pinacol coupling.<sup>25</sup> These reactions can occur enantioselectively<sup>26</sup> even under aqueous conditions.<sup>27</sup> We have recently extended the use of Cp<sub>2</sub>TiCl to radical polymer chemistry and demonstrated the first examples of an early transition metal catalyzed living radical polymerization of styrene initiated by epoxide RRO,<sup>28</sup> aldehyde SET reduction,<sup>29</sup> or peroxides.<sup>30</sup> The effect of ligands,<sup>31</sup> reducing agents,<sup>32</sup> solvents, and additives<sup>33</sup> as well as reagent ratios and temperature was also investigated. This study revealed the superiority of sandwich metallocenes over alkoxide and half-sandwich ligands and the relatively weak influence of the Cp substituents. Gratifyingly, the most promising catalyst (Cp<sub>2</sub>TiCl<sub>2</sub>) was also the least expensive one.<sup>34</sup> Furthermore, Ti alkoxides generated in situ by epoxide RRO catalyze the living ring-opening polymerization of cyclic esters.<sup>35</sup>

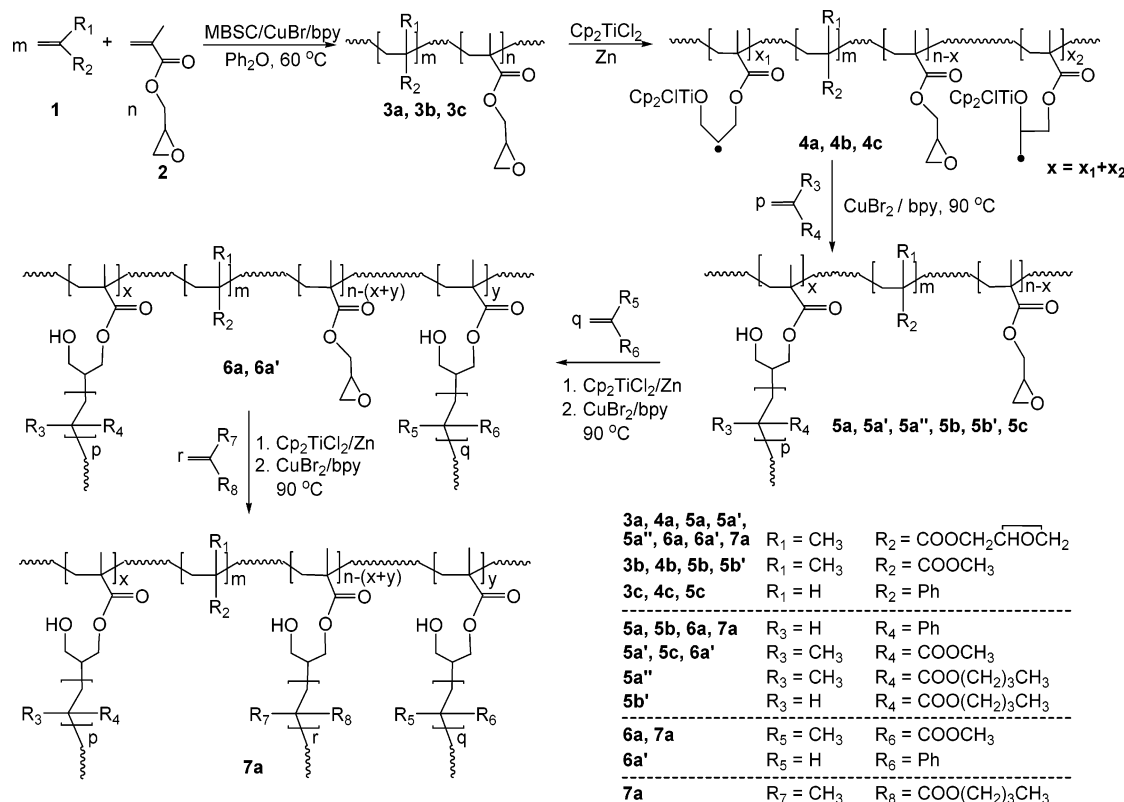
Typical LRP initiators for metal catalyzed polymerizations are based either on redox processes involving late transition metal complexes and activated alkyl halides or on thermal systems.<sup>14</sup> Thus, living grafting copolymerization by ATRP via the “grafting from” method requires the presence of activated halides along the polymer backbone. Consequently, the main chain cannot be synthesized directly in a controlled fashion via ATRP, unless the halide is masked<sup>36</sup> at the expense of the increase in the number of synthetic steps. Therefore, a wider

<sup>†</sup> Institute of Materials Science, Polymer Program.

<sup>‡</sup> Department of Chemistry.

\* Corresponding author: Ph 860-486-9062; Fax 860-486-4745; e-mail asandei@mail.ims.uconn.edu.

Scheme 1. Synthesis of PGMA-Based Graft Copolymers



assortment of ATRP-compatible initiator functionalities would greatly simplify and expand the usefulness of this method. As describe earlier, epoxides generate reactive radicals upon their  $\text{Cp}_2\text{TiCl}$  catalyzed radical ring opening. Moreover, well-defined epoxide macroinitiators derived from poly(glycidyl methacrylate) (PGMA) and its copolymers are easily accessible by ATRP<sup>37</sup> or from epoxidation of unsaturated polymers (e.g., poly(isoprene)).<sup>38</sup> Thus, we decided to explore the potential of the epoxide radical ring-opening reaction in “grafting from” processes. We are describing herein the first example of the use of epoxides in the synthesis of poly(styrene) and poly(alkyl (meth)acrylate) graft copolymers by radical graft copolymerizations initiated from PGMA and GMA copolymers with MMA and St. While related structures could conceivably be synthesized using less convenient anionic polymerizations and a “grafting onto” approach,<sup>38,39</sup> this novel protocol benefits from the much less stringent requirements associated with radical polymerizations and a much broader monomer selection. In addition, a sequential preparation of mixed arm graft copolymers is envisioned.

## Experimental Section

**Materials.** Glycidyl methacrylate (GMA, Acros, 97%), methyl methacrylate (MMA, Fisher, >98%), *n*-butyl methacrylate (BMA, 99%, Fluka), *n*-butyl acrylate (BA, 99+%), and styrene (St, 99+%, both from Aldrich) were dried over  $\text{CaH}_2$  (Acros) and passed through a basic  $\text{Al}_2\text{O}_3$  column. Bis(cyclopentadienyl)titanium dichloride ( $\text{Cp}_2\text{TiCl}_2$ , Acros, 97%) was recrystallized from  $\text{CH}_2\text{Cl}_2$ .  $\text{CuCl}$  (99.99%),  $\text{CuCl}_2$  (99%),  $\text{CuBr}_2$  (99+%), 4-methoxybenzenesulfonyl chloride (MBSC, 99%), ethyl 2-bromoisobutyrate (EBIB, 98%) *p*-toluenesulfonyl chloride (PTSCl, 99+%, all from Acros),  $\text{CuBr}$  (99.99%, Aldrich), Zn powder (100 mesh, 99.9%), diphenyl ether ( $\text{Ph}_2\text{O}$ , 98%, both from Alfa Aesar), 2,2'-bipyridyl (bpy, >99%, Fluka), methanol (99.9%, Fisher), tetrahydrofuran (99.9%, Fisher), and concentrated  $\text{H}_2\text{SO}_4$  (J.T. Baker) were used as received. Dioxane (99.7%, Acros) and anisole (99%, Acros) were distilled over Na/benzophenone.

**Techniques.**  $^1\text{H}$  NMR (500 MHz) spectra were recorded on a Bruker DRX-500 at 24 °C in  $\text{CDCl}_3$  (Aldrich; 0.03% v/v tetramethylsilane (TMS) as internal standard). GPC analyses were performed at 34 °C on a Waters 150-C Plus gel permeation chromatograph equipped with a Waters 410 differential refractometer, a Waters 2487 dual wavelength absorbance UV-vis detector set at 254 nm, a Polymer Laboratories PL-ELS 1000 evaporative light scattering (ELS) detector, and a Jordi Flash Gel  $10^5$  Å,  $2 \times 10^4$  Å, and  $1 \times 10^3$  Å column setup. THF (99.9% HPLC grade, Fisher) was used as eluent at a flow rate of 3 mL/min. Number-average ( $M_n$ ) and weight-average molecular weights ( $M_w$ ) were determined from calibration plots constructed with polystyrene standards. Differential scanning calorimetry (DSC) was performed on a TA Instruments (Q-100 series) DSC-2920 instrument calibrated with In and Zn standards. Typical sample sizes were between 10 and 15 mg. The samples were initially heated at 20 °C/min to 150 °C and annealed for 2 min at this temperature to remove thermal history. The samples were then cooled to -10 °C (for PBA containing samples, to -80 °C) at 40 °C/min and held there for 2 min, followed by a second heating at 20 °C/min up to 150 °C. Universal Analysis software (TA Instruments, version 4.2 E, build 4.2.0.38) was used to calculate  $T_g$  from the second heating curve of all polymers.

**Synthesis of Macroinitiators and Graft Copolymers. PGMA.**  $\text{CuBr}$  (43.0 mg, 0.30 mmol), bpy (141.0 mg, 0.90 mmol), and  $\text{Ph}_2\text{O}$  (4.0 mL) were added to a 25 mL Schlenk tube which was degassed by several freeze-pump-thaw cycles and was filled with Ar. GMA (4.0 mL, 30.11 mmol) and EBIB (44.2  $\mu\text{L}$ , 0.30 mmol) were injected, and the tube was redegassed and heated at 40 °C for 2 h. The polymer was precipitated into cold methanol, filtered, and dried.  $M_n = 16\,300$ ,  $M_w/M_n = 1.15$ ; 95% conversion.

**PGMA-co-PMMA.**  $\text{CuCl}$  (149.0 mg, 1.51 mmol), bpy (705.4 mg, 4.52 mmol), and  $\text{Ph}_2\text{O}$  (6.0 mL) were added to a 25 mL Schlenk tube which was degassed by several freeze-pump-thaw cycles and was filled with Ar. GMA (2.0 mL, 15.05 mmol), MMA (6.4 mL, 60.22 mmol), and MBSC (311.0 mg, 1.51 mmol) were injected, and the tube was redegassed and heated at 60 °C for 8 h. The polymer was precipitated into cold methanol, filtered, and dried.

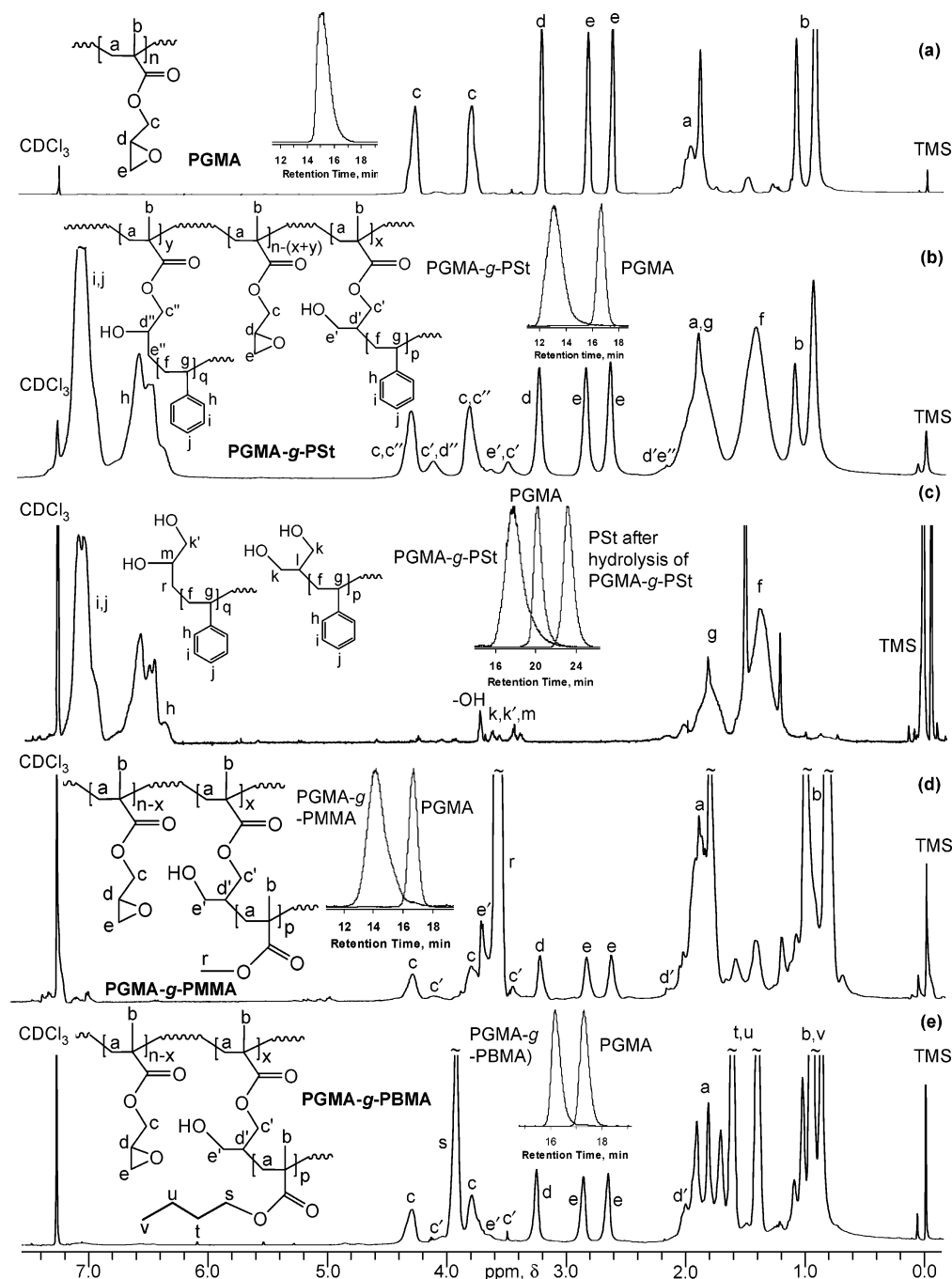


**Figure 1.** 500 MHz <sup>1</sup>H NMR spectra of (a) PGMA, (b) PGMA-g-PSt, (c) PSt derived from the hydrolysis of PGMA-g-PSt, (d) PGMA-g-PMMA, (e) PGMA-g-PBMA. Inset: GPC traces of PGMA and of the corresponding graft copolymers.

$M_n = 5800$ ,  $M_w/M_n = 1.11$ ; GMA conversion = 96% and MMA conversion = 97%; PGMA/PMMA = 20/80 (mol/mol).

**PGMA-co-PSt.** CuCl (35.5 mg, 0.35 mmol), bpy (168.0 mg, 1.07 mmol), and Ph<sub>2</sub>O (4.0 mL) were added to a 25 mL Schlenk tube which was degassed by several freeze–pump–thaw cycles and was filled with Ar. GMA (2.0 mL, 15.05 mmol), St (2.4 mL, 20.79 mmol), and PTSCl (68.3 mg, 0.35 mmol) were injected, and the tube was redegassed and heated at 120 °C for 15 h. The polymer was precipitated into cold methanol, filtered, and dried.  $M_n = 24\,674$ ,  $M_w/M_n = 1.34$ ; GMA conversion = 98% and St conversion = 91%; PGMA/PSt = 46/54 (mol/mol).

**Graft Copolymerization. PGMA-g-PSt.** Cp<sub>2</sub>TiCl<sub>2</sub> (17.5 mg, 0.07 mmol), Zn (2.5 mg, 0.04 mmol), and dioxane (1.0 mL) were added to a 25 mL Schlenk tube which was degassed by several freeze–pump–thaw cycles and filled with Ar, and the reduction was carried out at room temperature. The characteristic lime-green color of Ti(III) was observed in 10 min. The tube was then cooled

to –78 °C in an acetone/dry ice bath. A mixture of monomer (styrene, 0.8 mL, 7.03 mmol), macroinitiator (PGMA,  $M_n = 16\,300$ , PDI = 1.15, 0.2 g in 1 mL of dioxane), CuBr<sub>2</sub> (15.7 mg, 0.07 mmol), and bpy (33.0 mg, 0.21 mmol) was added under Ar, and the tube was redegassed and heated at 90 °C in an oil bath for 18 h. Samples were taken under Ar using an airtight syringe and were used for conversion and molecular weight determination by NMR and GPC, respectively. PGMA-g-PSt copolymer was precipitated into cold methanol, filtered, and dried.  $M_n = 46\,500$ ,  $M_w/M_n = 1.49$ ; St conversion = 53%; PGMA/PSt = 20/80 (mol/mol).

**PGMA-g-PMMA.** Cp<sub>2</sub>TiCl<sub>2</sub> (17.5 mg, 0.07 mmol), Zn (2.5 mg, 0.04 mmol), and dioxane (1.0 mL) were added to a 25 mL Schlenk tube which was degassed by several freeze–pump–thaw cycles and filled with Ar, and the reduction was carried out at room temperature. The characteristic lime-green color of Ti(III) was observed in 10 min. The tube was then cooled to –78 °C in an acetone/dry ice bath. A mixture of monomer (MMA, 0.8 mL, 7.03



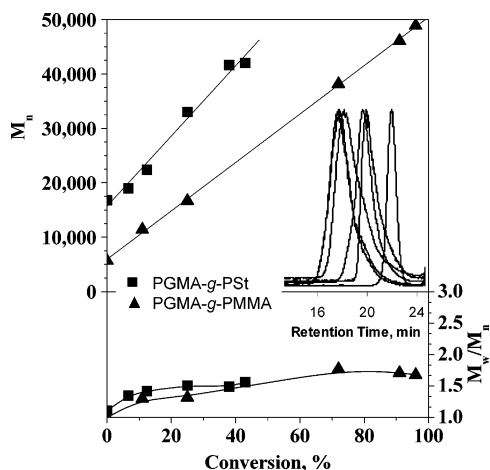


**Figure 2.** Dependence of  $M_n$  and  $M_w/M_n$  on conversion in  $\text{CuBr}_2$ -mediated graft copolymerization of MMA and St initiated by  $\text{Cp}_2\text{TiCl}_2$  catalyzed PGMA epoxide RRO: MMA ( $\blacktriangle$  and GPC inset;  $[\text{GMA}]/[\text{MMA}]/[\text{Cp}_2\text{TiCl}_2]/[\text{Zn}]/[\text{CuBr}_2]/[\text{bpy}] = 100/500/5/2.75/5/15$ ,  $T = 90^\circ\text{C}$ ); St ( $\blacksquare$ ,  $[\text{GMA}]/[\text{St}]/[\text{Cp}_2\text{TiCl}_2]/[\text{Zn}]/[\text{CuBr}_2]/[\text{bpy}] = 100/500/5/2.75/5/15$ ,  $T = 90^\circ\text{C}$ ).

mmol), macroinitiator (PGMA,  $M_n = 6400$ , PDI = 1.12, 0.2 g in 1 mL of dioxane),  $\text{CuBr}_2$  (15.7 mg, 0.07 mmol), and bpy (33.0 mg, 0.21 mmol) was added under Ar, and the tube was redegassed and heated at  $90^\circ\text{C}$  for 4 h. Samples were taken under Ar using an airtight syringe and were used for conversion and molecular weight determination by NMR and GPC, respectively. PGMA-g-PMMA was precipitated into cold methanol, filtered, and dried.  $M_n = 39\,868$ ,  $M_w/M_n = 1.40$ ; MMA conversion = 91%; PGMA/PMMA = 10/90 (mol/mol).

**PGMA-g-PBMA.**  $\text{Cp}_2\text{TiCl}_2$  (6.3 mg, 0.02 mmol), Zn (0.8 mg, 0.01 mmol), and dioxane (1.0 mL) were added to a 25 mL Schlenk tube which was degassed by several freeze–pump–thaw cycles and filled with Ar, and the reduction was carried out at room temperature. The characteristic lime-green color of Ti(III) was observed in 10 min. The tube was then cooled to  $-78^\circ\text{C}$  in an acetone/dry ice bath. A mixture of monomer (BMA, 0.4 mL, 2.53 mmol), macroinitiator (PGMA,  $M_n = 6400$ , PDI = 1.12, 0.2 g in 1 mL of dioxane),  $\text{CuCl}_2$  (3.4 mg, 0.02 mmol), and bpy (9.9 mg, 0.06 mmol) was added under Ar, and the tube was redegassed and heated at  $90^\circ\text{C}$  for 22 h. The copolymer was precipitated into cold methanol, filtered, and dried.  $M_n = 58\,073$ ,  $M_w/M_n = 1.34$ ; BMA conversion = 88%; PGMA/PBMA = 15/85 (mol/mol).

**(PGMA-co-PMMA)-g-PSt.**  $\text{Cp}_2\text{TiCl}_2$  (23.9 mg, 0.09 mmol), Zn (3.2 mg, 0.05 mmol), and dioxane (1.0 mL) were added to a 25 mL Schlenk tube which was degassed by several freeze–pump–thaw cycles and filled with Ar, and the reduction was carried out at room temperature. The characteristic lime-green color of Ti(III) was observed in 10 min. The tube was then cooled to  $-78^\circ\text{C}$  in an acetone/dry ice bath. A mixture of monomer (St, 1.1 mL, 9.63 mmol), macroinitiator (PGMA-co-PMMA,  $M_n = 5800$ , PDI = 1.11, PGMA/PMMA = 20/80, 0.2 g in 1 mL of dioxane),  $\text{CuBr}_2$  (21.5 mg, 0.09 mmol), and bpy (45.1 mg, 0.28 mmol) was added under Ar, and the tube was redegassed and heated at  $80^\circ\text{C}$  in an oil bath for 9 h. Samples were taken under Ar using an airtight syringe and used for conversion and molecular weight determination by NMR and GPC, respectively. (PGMA-co-PMMA)-g-PSt was precipitated into cold methanol, filtered, and dried.  $M_n = 10\,406$ ,  $M_w/M_n = 1.55$ ; St conversion = 25%; PGMA/PMMA/PSt = 15/55/30 (mol/mol).

**(PGMA-co-PMMA)-g-PBA.**  $\text{Cp}_2\text{TiCl}_2$  (9.8 mg, 0.04 mmol), Zn (1.4 mg, 0.02 mmol), and dioxane (0.5 mL) were added to a 25 mL Schlenk tube which was degassed by several freeze–pump–thaw cycles and filled with Ar, and the reduction was carried out at room temperature. The characteristic lime-green color of Ti(III) was observed in 10 min. The tube was then cooled to  $-78^\circ\text{C}$  in an acetone/dry ice bath. A mixture of monomer (BA, 0.2 mL, 1.98 mmol), macroinitiator (PGMA-co-PMMA,  $M_n = 5500$ , PDI = 1.14,

PGMA/PMMA = 2/98, 0.2 g in 1 mL of dioxane),  $\text{CuBr}_2$  (17.6 mg, 0.08 mmol), and bpy (37.1 mg, 0.24 mmol) was added under Ar, and the tube was redegassed and heated at  $90^\circ\text{C}$  in an oil bath for 10 h. (PGMA-co-PMMA)-g-PBA was precipitated into cold methanol, filtered, and dried.  $M_n = 8900$ ,  $M_w/M_n = 1.07$ ; BA conversion = 23%; PGMA/PMMA/PBA = 1.8/91/7.2 (mol/mol/mol).

**(PGMA-co-PSt)-g-PMMA.**  $\text{Cp}_2\text{TiCl}_2$  (15.1 mg, 0.06 mmol), Zn (2.0 mg, 0.03 mmol), and anisole (1.0 mL) were added to a 25 mL Schlenk tube which was degassed by several freeze–pump–thaw cycles and filled with Ar, and the reduction was carried out at room temperature. The characteristic lime-green color of Ti(III) was observed in 10 min. The tube was then cooled to  $-78^\circ\text{C}$  in an acetone/dry ice bath. A mixture of monomer (MMA, 0.5 mL, 4.57 mmol), macroinitiator (PGMA-co-PSt,  $M_n = 24\,674$ , PDI = 1.34, PGMA/PSt = 46/54, 0.3 g in 1 mL of anisole),  $\text{CuCl}_2$  (8.2 mg, 0.06 mmol), and bpy (23.8 mg, 0.15 mmol) was added under Ar, and the tube was redegassed and heated at  $75^\circ\text{C}$  in an oil bath for 18 h. (PGMA-co-PSt)-g-PMMA was precipitated into cold methanol, filtered, and dried.  $M_n = 42\,121$ ,  $M_w/M_n = 1.70$ ; MMA conversion = 67%; PGMA/PSt/PMMA = 25/30/45 (mol/mol/mol).

**Sequential Graft Copolymerization. (PGMA-g-PMMA)-g-PSt.**  $\text{Cp}_2\text{TiCl}_2$  (2.4 mg, 0.009 mmol), Zn (0.3 mg, 0.005 mmol), and dioxane (0.5 mL) were added to a 25 mL Schlenk tube which was degassed by several freeze–pump–thaw cycles and filled with Ar, and the reduction was carried out at room temperature. The characteristic lime-green color of Ti(III) was observed in 10 min. The tube was then cooled to  $-78^\circ\text{C}$  in an acetone/dry ice bath. A mixture of monomer (styrene, 0.5 mL, 4.86 mmol), macroinitiator (PGMA-g-PMMA,  $M_n = 39\,868$ , PDI = 1.41, PGMA/PMMA = 10/90, 84% unopened PGMA epoxide, 0.2 g in 1 mL of dioxane),  $\text{CuBr}_2$  (2.2 mg, 0.009 mmol), and bpy (4.6 mg, 0.03 mmol) was added under Ar, and the tube was redegassed and heated at  $90^\circ\text{C}$  in an oil bath for 19 h. (PGMA-g-PMMA)-g-PSt was precipitated into cold methanol, filtered, and dried.  $M_n = 49\,502$ ,  $M_w/M_n = 1.43$ ; St conversion = 16%; PGMA/PMMA/PSt = 6/58/36 (mol/mol/mol).

**(PGMA-g-PSt)-g-PMMA.**  $\text{Cp}_2\text{TiCl}_2$  (3.4 mg, 0.013 mmol), Zn (0.5 mg, 0.007 mmol), and dioxane (0.5 mL) were added to a 25 mL Schlenk tube which was degassed by several freeze–pump–thaw cycles and filled with Ar, and the reduction was carried out at room temperature. The characteristic lime-green color of Ti(III) was observed in 10 min. The tube was then cooled to  $-78^\circ\text{C}$  in an acetone/dry ice bath. A mixture of monomer (MMA, 0.7 mL, 6.81 mmol), macroinitiator (PGMA-g-PSt,  $M_n = 83\,000$ , PDI = 1.57, PGMA/PSt = 8/92, 83% unopened PGMA epoxide, 0.4 g in 1.5 mL of dioxane),  $\text{CuBr}_2$  (3.0 mg, 0.013 mmol), and bpy (6.4 mg, 0.04 mmol) was added under Ar, and the tube was redegassed and heated at  $90^\circ\text{C}$  in an oil bath for 24 h. (PGMA-g-PSt)-g-PMMA was precipitated into cold methanol, filtered, and dried.  $M_n = 102\,967$ ,  $M_w/M_n = 1.48$ ; MMA conversion = 35%; PGMA/PSt/PMMA = 5/68/27 (mol/mol/mol).

**((PGMA-g-PMMA)-g-PSt)-g-PBMA.**  $\text{Cp}_2\text{TiCl}_2$  (9.0 mg, 0.03 mmol), Zn (2.3 mg, 0.03 mmol), and dioxane (0.5 mL) were added to a 25 mL Schlenk tube which was degassed by several freeze–pump–thaw cycles and filled with Ar, and the reduction was carried out at room temperature. The characteristic lime-green color of Ti(III) was observed in 10 min. The tube was then cooled to  $-78^\circ\text{C}$  in an acetone/dry ice bath. A mixture of monomer (BMA, 1.1 mL, 7.27 mmol), macroinitiator ((PGMA-g-PMMA)-g-PSt,  $M_n = 49\,502$ , PDI = 1.43, PGMA/PMMA/PSt = 6/58/36, 63% unopened PGMA epoxide, 0.1 g in 1.0 mL of dioxane),  $\text{CuBr}_2$  (8.1 mg, 0.03 mmol), and bpy (17.0 mg, 0.11 mmol) was added under Ar, and the tube was redegassed and heated at  $90^\circ\text{C}$  in an oil bath for 42 h. ((PGMA-g-PMMA)-g-PSt)-g-PBMA was precipitated into cold methanol, filtered, and dried.  $M_n = 245\,161$ ,  $M_w/M_n = 2.09$ ; BMA conversion > 99%; PGMA/PMMA/PSt/PBMA = 1/10/6.4/82.6 (mol/mol/mol/mol).

**Graft Copolymer Hydrolysis.** 0.05 g of polymer (PGMA-g-PSt, PGMA/PSt = 20/80,  $M_n = 46\,500$ ; PDI = 1.49) was dissolved in 10 mL of THF in a 50 mL Schlenk tube. 10 drops of concentrated sulfuric acid was added into it, and the mixture was refluxed at

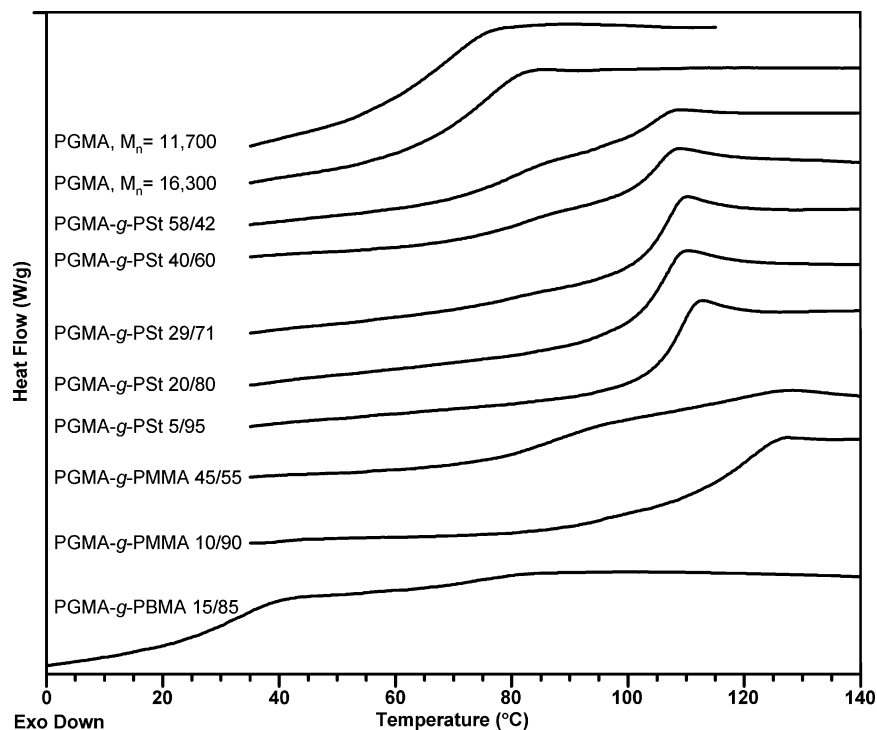


**Figure 3.** Selected DSC traces of PGMA, PGMA-g-PSt, PGMA-g-PMMA, and PGMA-g-PBMA.

100 °C for 7 days. The solvent was removed under vacuum, and the remaining solid was dissolved in a mixture of water and CH<sub>2</sub>-Cl<sub>2</sub>. The organic layer was extracted three times from water, combined, and dried over MgSO<sub>4</sub>. The solution was then concentrated and precipitated in methanol. The solid polymer was dried under vacuum overnight and characterized by <sup>1</sup>H NMR and GPC.  $M_n = 2000$ ,  $M_w/M_n = 1.15$ .

## Results and Discussion

The synthesis of linear and graft copolymers is outlined in Scheme 1. The results are presented in Figures 1–7 and summarized in Tables 1–3. Narrow polydispersity linear PGMA, PGMA-co-PMMA, and PGMA-co-PSt (**3a**, **3b**, **3c**) macroinitiators of various molecular weights were synthesized by ATRP using MBSC, EBIB, or PTSCl as initiators and CuCl/bpy or CuBr/bpy as the catalyst/ligand system.<sup>37</sup> The grafting procedure involves the in-situ generation of Cp<sub>2</sub>TiCl followed by the injection of a mixture of macroinitiator, grafting monomer, and CuBr<sub>2</sub>/bpy. The characteristic green color of Cp<sub>2</sub>TiCl develops within 5–10 min upon stirring the red Cp<sub>2</sub>TiCl<sub>2</sub> with Zn at room temperature. Injection of a PGMA/monomer solution into the Cp<sub>2</sub>TiCl solution leads to a rapid color change to red-orange, indicating the consumption of Cp<sub>2</sub>TiCl by epoxide radical ring opening (RRO). The RRO proceeds with the formation of macromolecular Ti alkoxides (Cp<sub>2</sub>CITi–O–PGMA) and of a mixture of reactive, constitutionally isomeric primary and secondary C-centered radicals derived from the regioselectivity of the RRO (**4a**, **4b**, **4c**). The β-titanoxy radicals have the same thermodynamic stabilization as the corresponding alkyl radicals,<sup>40</sup> and typically the secondary radical is favored.

Such radicals add readily to conventional monomers such as (meth)acrylates<sup>41</sup> and styrene<sup>28–34</sup> and initiate the polymerization. For simplicity, only the more favored mode of epoxide RRO is depicted in Scheme 1 for the grafted structures. The GMA macroinitiators typically contain a large excess of epoxide groups by comparison with available Cp<sub>2</sub>TiCl and thus lead to its fast and complete consumption. Therefore, other LRP mediators such as CuX<sub>2</sub> (X = Cl, Br) or nitroxides are required

to control grafting and prevent potential cross-linking. Two potential side reactions are envisioned, but as described later, they do not appear to significantly interfere with the grafting. First, it is conceivable that Zn or Cp<sub>2</sub>TiCl may reduce CuBr<sub>2</sub>. However, Zn is used in only stoichiometric amounts vs Cp<sub>2</sub>TiCl<sub>2</sub> and is completely consumed prior to the addition of the other starting materials. Moreover, the large excess of epoxide/Cp<sub>2</sub>TiCl and the high reactivity of Cp<sub>2</sub>TiCl toward epoxide RRO<sup>23</sup> leads to the almost instantaneous consumption of all available Cp<sub>2</sub>TiCl, as evidenced by instant color change from green to red/orange. Second, CuBr<sub>2</sub> could possibly transfer bromine to the epoxide-derived radicals and generate inactivated halides. However, the addition of the initiating radicals to the double bonds is apparently very fast even at low temperature, and this process does not affect the initiation. Since the PGMA macroinitiators were synthesized by ATRP, the terminal halide can also act as an additional initiator in the presence of Cu(I), but the concentration of the chain ends is much smaller than that of the available epoxides. Thus, after the Ti-mediated RRO initiation, CuX<sub>2</sub>/bpy enables the synthesis of the graft copolymers (**5**) in a controlled fashion, following a reverse ATRP<sup>42</sup> mechanism. While the optimization of the process and the in-depth study of the effect of stoichiometry are in progress, a Cp<sub>2</sub>TiCl<sub>2</sub>/Zn/CuBr<sub>2</sub> = 1/0.5/1 ratio was used in all experiments. Moreover, the RRO of only a part of the available epoxides during grafting enables the *sequential* grafting copolymerization of several different monomers (**6**, **7**) until the complete consumption of all epoxides. Architectural variables such as graft density and length can be manipulated from the monomer/Cp<sub>2</sub>TiCl/epoxide ratios and from the composition of the main chain GMA-based macroinitiator.

**Grafting from PGMA.** The characterization of graft copolymers derived from PGMA is summarized in Table 1. The occurrence of grafting is supported by a combination of NMR, GPC, and DSC. A comparison of the 500 MHz <sup>1</sup>H NMR spectra of PGMA, PGMA-g-PSt (**5a**), PGMA-g-PMMA (**5a'**), and PGMA-g-PBMA (**5a''**) is provided in Figure 1. As expected,

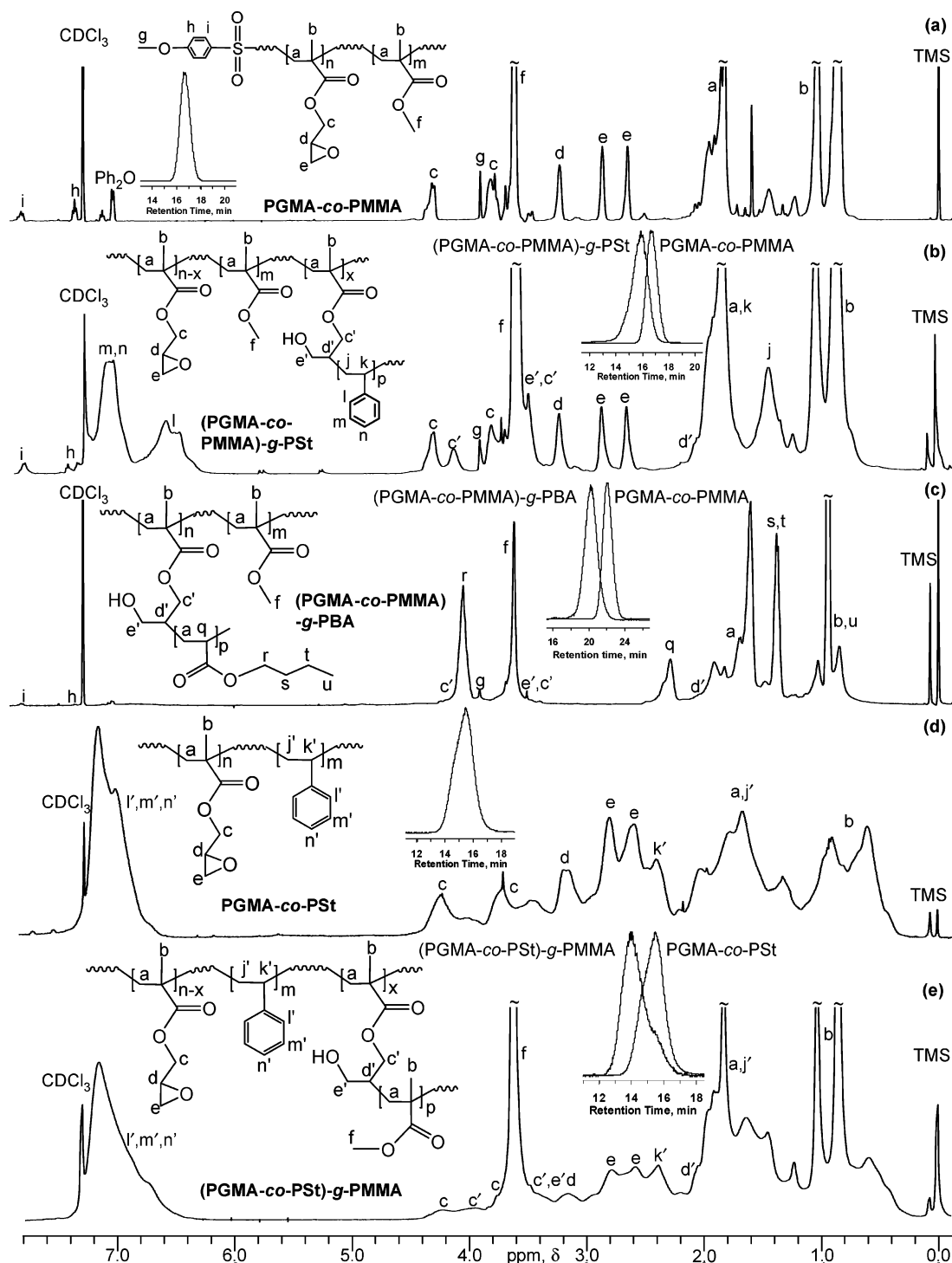


**Figure 4.** 500 MHz  $^1\text{H}$  NMR spectra of (a) PGMA-co-PMMA, (b) (PGMA-co-PMMA)-g-PSt, (c) (PGMA-co-PMMA)-g-PBA, (d) PGMA-co-PSt, and (e) (PGMA-co-PSt)-g-PMMA. Inset: GPC traces of macroinitiators and of the graft copolymers.

the graft copolymer spectra contain resonances from the parent PGMA such as  $a$  ( $-\text{CH}_2-$ ) and  $b$  ( $-\text{CH}_3$ ) of the main chain,  $c$ ,  $d$ ,  $e$  of the unopened epoxide, and  $c'$ ,  $c''$ ,  $d'$ ,  $d''$ ,  $e'$ ,  $e''$  corresponding to the two paths of epoxide opening. For simplicity, both modes of RRO are drawn only for PGMA-g-PSt but are envisioned in all other cases below. In addition, resonances associated with the grafted copolymers such as PSt (aliphatic  $f$ ,  $g$  and aromatic  $h$ ,  $i$ ,  $j$ ), PMMA ( $a$ ,  $b$ , and  $r$  of  $\text{OCH}_3$ ), and PBMA ( $a$ ,  $b$  and  $s$ ,  $t$ ,  $u$ ,  $v$  of  $n$ -butyl) are also present. The NMR data allow the estimation of graft density (% RRO) and copolymer composition. If there was no overlap between the epoxide and other resonances (e.g., styrene grafting), % RRO

was determined from the integration of opened and unopened epoxides (e.g., Figure 1b, % RRO =  $100(c' + c'')/(c' + c'' + c)$ ). Alternatively, for methacrylates, % RRO was obtained by comparing the remaining unopened epoxides with the main chain PGMA methyl group (e.g., Figure 1d: % RRO =  $(1 - d/(b/3 - r/3)) \times 100$ ). Accordingly, in most cases, as expected from the  $\text{Cp}_2\text{TiCl}/\text{epoxide}$  ratios (Table 1) about 20% of the epoxide groups were opened. This indicates a graft density of about one chain at every five GMA units and a graft length of about 4–140 units. The graft length increases with the monomer/GMA ratio and conversion. However, since the polymerizations were stopped at different conversions, the

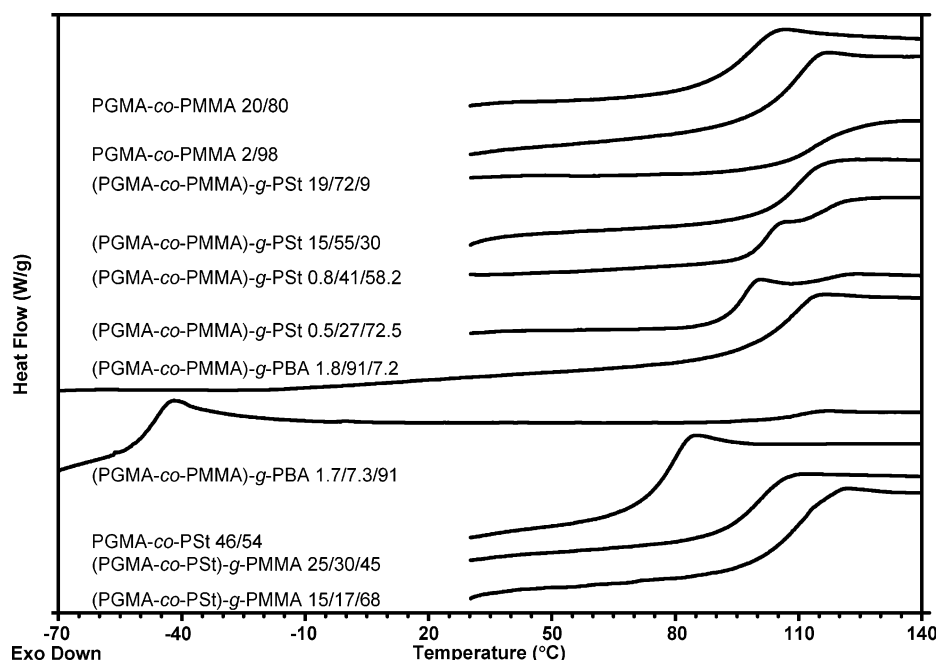


**Figure 5.** Selected DSC traces of PGMA-co-PMMA, (PGMA-co-PMMA)-g-PSt, (PGMA-co-PMMA)-g-PBA, PGMA-co-PSt, and (PGMA-co-PSt)-g-PMMA.

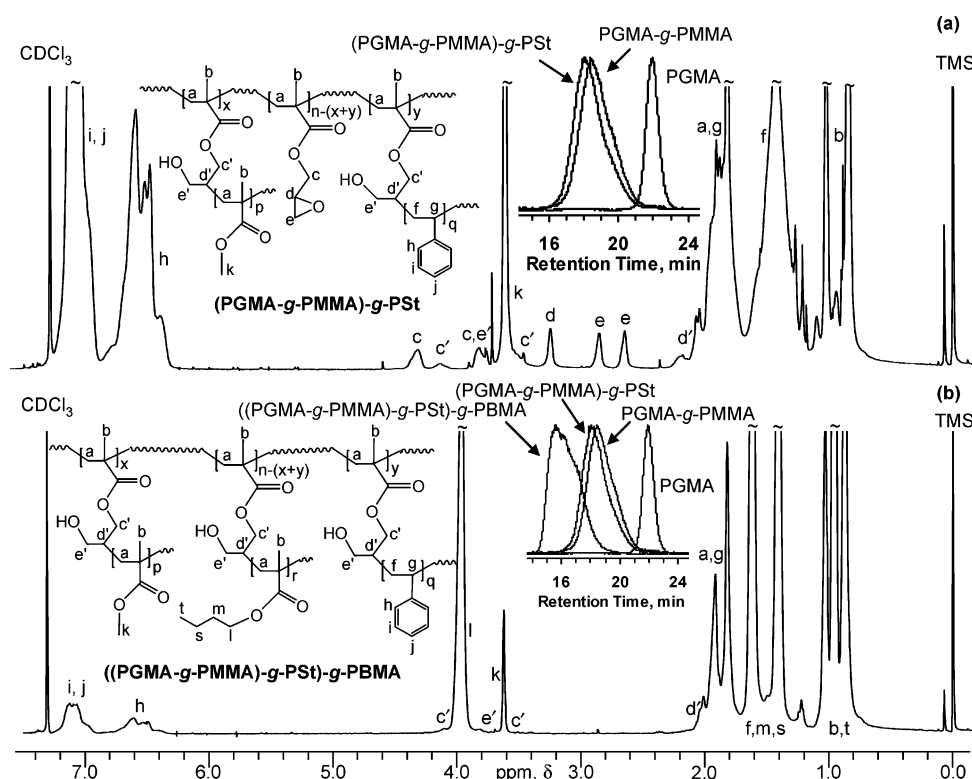


**Figure 6.** 500 MHz <sup>1</sup>H NMR spectra of (a) (PGMA-g-PMMA)-g-PSt and (b) ((PGMA-g-PMMA)-g-PSt)-g-PBMA. Inset: GPC traces of macroinitiators and of the graft copolymers.

molecular weight increase upon grafting does not scale directly with the initial monomer/GMA ratio. Thus, the experiments in Table 1 are listed according to the final copolymer composition.

Hydrolysis of the side chain GMA ester linkage in the graft copolymers was used to further confirm the grafting process. Thus, acid-catalyzed hydrolysis of PGMA-g-PSt ( $M_n = 46\,500$ ,  $M_w/M_n = 1.49$ ; Table 1, experiment 4) produces poly(methacrylic acid) and diol-terminated polystyrene ( $M_n = 2000$ ;  $M_w/M_n = 1.15$ ). The PSt NMR spectrum also included in Figure

1 enables determination of the average PSt graft length and of the regioselectivity of the epoxide RRO. Initiation from the GMA epoxides is demonstrated by the characteristic resonances of the diol chain end which is derived from the PGMA ester hydrolysis and from a combination of the two modes of epoxide RRO ( $-OH$ ,  $\delta = 3.68$  ppm,  $-CH-(CH_2-OH)_2$  and  $-CH(OH)-CH_2OH$ ,  $\delta = 3.33-3.63$  ppm). Accordingly,  $M_n^{NMR} \sim 2300$ , and as expected, the epoxide ring opens predominantly with the formation of the more stable secondary vs primary radical by an approximate ratio of 75/25.

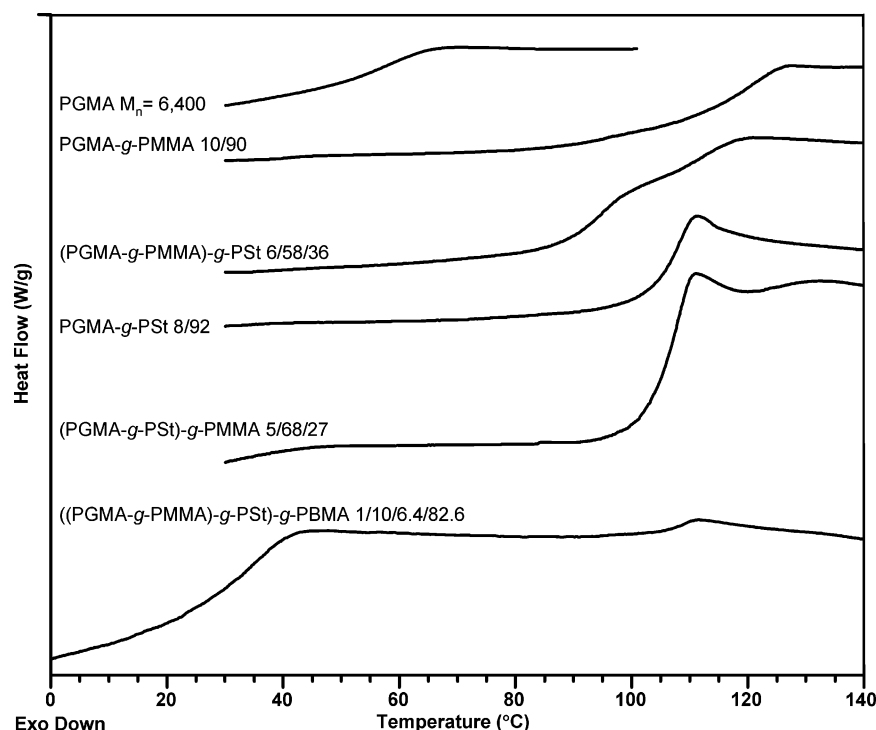


**Figure 7.** Selected DSC traces of PGMA, PGMA-*g*-PMMA, (PGMA-*g*-PMMA)-*g*-PSt, PGMA-*g*-PSt, (PGMA-*g*-PSt)-*g*-PMMA, and ((PGMA-*g*-PMMA)-*g*-PSt)-*g*-PBMA.

**Table 1.**  $\text{Cp}_2\text{TiCl/CuBr}_2$  Catalyzed Graft Copolymerization of St, MMA, and BMA from PGMA

| expt | $M_1$ | $\text{GMA}/M_1^a$ | $T$ (°C) | $t$ (h) | $M_1$ conv (%) <sup>b</sup> | RRO (%) <sup>b</sup> | PGMA               |            | PGMA- <i>g</i> -PM <sub>1</sub> |                                   |            |
|------|-------|--------------------|----------|---------|-----------------------------|----------------------|--------------------|------------|---------------------------------|-----------------------------------|------------|
|      |       |                    |          |         |                             |                      | $M_n$<br>$M_w/M_n$ | $T_g$ (°C) | $M_n$<br>$M_w/M_n$              | PGMA/PM <sub>1</sub> <sup>b</sup> | $T_g$ (°C) |
| 1    | St    | 100/125            | 80       | 72      | 57                          | 19                   | 11700<br>1.16      | 66         | 17300<br>1.70                   | 58/42                             | 77<br>104  |
| 2    | St    | 100/500            | 90       | 6       | 26                          | 22                   | 16300<br>1.15      | 72         | 31100<br>1.66                   | 40/60                             | 76<br>104  |
| 3    | St    | 100/500            | 80       | 70      | 60                          | 25                   | 16300<br>1.15      | 72         | 44600<br>1.56                   | 29/71                             | 77<br>105  |
| 4    | St    | 100/500            | 90       | 18      | 53                          | 22                   | 16300<br>1.15      | 72         | 46500<br>1.49                   | 20/80                             | 104        |
| 5    | St    | 100/2000           | 80       | 23      | 47                          | 17                   | 6400<br>1.12       | 55         | 83000<br>1.57                   | 8/92                              | 106        |
| 6    | St    | 100/375            | 90       | 46      | 71                          | 13                   | 16300<br>1.15      | 72         | 41400<br>1.65                   | 5/95                              | 106        |
| 7    | MMA   | 100/150            | 60       | 25      | 49                          | 27                   | 13800<br>1.10      | 65         | 24701<br>1.32                   | 45/55                             | 84<br>118  |
| 8    | MMA   | 100/500            | 90       | 4       | 91                          | 16                   | 6400<br>1.12       | 55         | 39868<br>1.40                   | 10/90                             | 114        |
| 9    | BMA   | 100/200            | 90       | 22      | 88                          | 21                   | 6400<br>1.12       | 55         | 58073<br>1.34                   | 15/85                             | 30<br>76   |

<sup>a</sup> Calculated as  $\text{GMA}/M_1$  monomer mole ratio;  $[\text{PGMA}]/[\text{Cp}_2\text{TiCl}_2]/[\text{Zn}]/[\text{CuBr}_2]/[\text{bpy}] = 100/5/2.75/5/15$  (expt 9,  $[\text{PGMA}]/[\text{Cp}_2\text{TiCl}_2]/[\text{Zn}]/[\text{CuCl}_2]/[\text{bpy}] = 100/2/1/2/5$ ). <sup>b</sup> Determined by  $^1\text{H}$  NMR.

The GPC traces of PGMA graft copolymers (Figure 1, inset) show a monomodal increase in molecular weight from the parent PGMA. While  $M_n$  is measured vs linear PSt standards and is thus approximate, GPC in conjunction with the NMR results supports the formation of graft copolymers. Moreover, the use of  $\text{CuBr}_2/\text{bpy}$  enables control of the polymerization by reverse ATRP, and grafting occurs in a controlled fashion for both St and MMA, as shown in Figure 2. Accordingly, the graft copolymer molecular weight increases linearly with conversion and maintains a reasonable polydispersity of about 1.5–1.7 for PGMA-*g*-PSt and 1.3–1.5 for PGMA-*g*-PMMA and PGMA-*g*-PBMA.

The formation of graft copolymers is also supported by the DSC thermal characterization (Figure 3). PGMA-*g*-PSt copolymers with  $\text{GMA}/\text{St} = 58/42$  and  $40/60$  display two glass

transitions, as expected for immiscible systems.  $T_g^{\text{PGMA}}$  increases slightly from about 66–72 °C to about 77 °C, whereas  $T_g^{\text{PSt}} = 104$  °C, although  $\text{DP}_{\text{theor}}^{\text{PSt}}$  is only about 3–9 units. This is a consequence of the graft connectivity, which reduces the number of free PSt chain ends and restricts the PGMA backbone mobility while providing bulky PSt side groups. A minor shoulder is observed for the  $\text{GMA}/\text{St} = 29/71$  copolymer at 77 °C, while  $T_g^{\text{PGMA}}$  was not evident in copolymers with over 80% styrene.

Two different  $T_g$  values were also detected for PGMA-*g*-PMMA with a 45/55 composition. While alkyl methacrylates are typically miscible, this effect may be due to the larger polarity of the epoxide ring of the glycidyl group of GMA by comparison to the  $\text{CH}_3$  unit of MMA (e.g.,  $\mu = 1.89$  D for



Table 2. Cp<sub>2</sub>TiCl/CuBr<sub>2</sub> Catalyzed Graft Copolymerization of St, BA, and MMA from PGMA-co-PMMA and PGMA-co-PSt

| expt            | M <sub>1</sub> | M <sub>2</sub> | GMA/M <sub>1</sub> /M <sub>2</sub> /<br>Cp <sub>2</sub> TiCl <sub>2</sub> /Zn/<br>CuBr <sub>2</sub> /bpy | T (°C) | t (h) | M <sub>2</sub> conv<br>(%) <sup>a</sup> | RRO<br>(%) <sup>a</sup> | PGMA-co-PM <sub>1</sub>                          |                     | (PGMA-co-PM <sub>1</sub> )-g-PM <sub>2</sub>     |   |                     |
|-----------------|----------------|----------------|--|--------|-------|---|-------------------------|--|---------------------|--|---|---------------------|
|                 |                |                |  |        |       |   |                         | M <sub>n</sub><br>M <sub>w</sub> /M <sub>n</sub> | T <sub>g</sub> (°C) | M <sub>n</sub><br>M <sub>w</sub> /M <sub>n</sub> | GMA/M <sub>1</sub> /M <sub>2</sub> <sup>a</sup> | T <sub>g</sub> (°C) |
| 1               | MMA            | St             | 20/80/525/<br>5/2.75/5/15  | 80     | 9     | 25                                      | 38                      | 5800<br>1.11                                     | 95                  | 10406<br>1.55                                    | 15/55/30  | 107                 |
| 2               | MMA            | St             | 20/80/525/<br>21/10/21/63  | 80     | 9     | 20                                      | 82                      | 5800<br>1.11                                     | 95                  | 11472<br>1.42                                    | 19/72/9   | 113                 |
| 3               | MMA            | St             | 2/98/200/<br>4/8/0/0   | 90     | 7     | 54                                      | 100                     | 5346<br>1.12                                     | 106                 | 17407<br>2.33                                    | 0.8/41/58.2                                     | 101                 |
| 4               | MMA            | St             | 2/98/400/<br>4/8/0/0   | 90     | 46    | 62                                      | 100                     | 5698<br>1.06                                     | 106                 | 13532<br>2.82                                    | 0.5/21/78.5                                     | 116                 |
| 5               | MMA            | St             | 2/98/200/<br>6/12/0/0  | 75     | 20    | 77                                      | 100                     | 5698<br>1.06                                     | 106                 | 9051<br>1.39                                     | 0.5/27/72.5                                     | 97                  |
| 6               | MMA            | BA             | 2/98/100/<br>2/1/4/12  | 90     | 10    | 23                                      | 100                     | 5500<br>1.14                                     | 106                 | 8900<br>1.07                                     | 1.8/91/7.2                                      | 106                 |
| 7               | MMA            | BA             | 20/80/500<br>20/11/0/0   | 90     | 22    | 72                                      | 100                     | 5800<br>1.11                                     | 95                  | 21518<br>2.18                                    | 8.5/34/57.5                                     | -47                 |
| 8               | MMA            | BA             | 20/80/500<br>20/10/20/60   | 90     | 14    | 20                                      | 100                     | 5800<br>1.11                                     | 95                  | 14165<br>1.34                                    | 4.3/17.2/78.5                                   | -47                 |
| 9               | MMA            | BA             | 20/80/4000<br>20/11/0/0  | 90     | 24    | 96                                      | 100                     | 5800<br>1.11                                     | 95                  | 83409<br>1.99                                    | 1.7/7.3/91                                      | -48                 |
| 10 <sup>b</sup> | St             | MMA            | 46/54/187/<br>2.5/1.3/2.5/6.3  | 75     | 18    | 67                                      | 17                      | 24674<br>1.34                                    | 76                  | 42121<br>1.70                                    | 25/30/45  | 98                  |
| 11 <sup>b</sup> | St             | MMA            | 46/54/250/<br>2.5/1.3/2.5/6.3  | 90     | 19    | 85                                      | 22                      | 24674<br>1.34                                    | 76                  | 54121<br>1.67                                    | 15/17/68  | 108                 |

<sup>a</sup> Determined by <sup>1</sup>H NMR. <sup>b</sup> CuCl<sub>2</sub> was used instead of CuBr<sub>2</sub> in expts 10 and 11.

ethylene oxide and  $\mu \sim 0$  D for CH<sub>4</sub>).<sup>43</sup> Nonetheless, at higher MMA content (90%), a single glass transition,  $T_g = 118$  °C, is observed. PGMA-g-PBMA (15/85) displays a lower  $T_g$  at ~30 °C, which corresponds to the PBMA graft and a higher  $T_g$  at 76 °C associated with PGMA.

**Grafting from PGMA Copolymers.** GMA is a very reactive monomer that easily undergoes copolymerization with acrylates<sup>37,44</sup> or styrene<sup>45</sup> over a wide composition range. Consequently, the epoxide grafting methodology was also tested on GMA copolymers. Copolymerization dilutes the epoxide content and provides additional means of controlling graft density. The reactivity ratios of GMA and MMA ( $r_{\text{GMA}} = 0.94$ ,  $r_{\text{MMA}} = 0.75$ )<sup>46</sup> favor copolymers with similar compositions to comonomer feed. In the case of PGMA-co-PSt, the feed ratios were calculated according to the desired copolymer composition ( $r_{\text{GMA}} = 0.56$ ,  $r_{\text{St}} = 0.44$ ).<sup>45</sup> Although the ATRP of GMA can be performed at 60 °C, styrene polymerization is slow. Thus, to avoid formation of PGMA blocks, the copolymerization was carried out at 120 °C. The synthesis of random PGMA-co-PSt was supported by NMR via the characteristic broadening of the aliphatic resonances and the merger of the aromatic peaks.<sup>45</sup> PGMA-co-PMMA was also synthesized by ATRP, while the grafting was conducted as described for PGMA.

The characterization of PGMA-co-PMMA (**3b**) and PGMA-co-PSt (**3c**) linear macroinitiators and of the corresponding (PGMA-co-PMMA)-g-PSt (**5b**), (PGMA-co-PMMA)-g-PBA (**5b'**), and (PGMA-co-PSt)-g-PMMA (**5c**) graft copolymers is summarized in Table 2. A comparison of the 500 MHz <sup>1</sup>H NMR spectra of the linear and grafted structures is provided in Figure 4 and, as before, permits the evaluation of composition, % epoxide ring opening, and graft length. Thus, upon grafting, new aromatic styrene resonances (*l*, *m*, *n*) as well as aliphatic butyl resonances (*r*, *s*, *t*, *u*) are observed in the spectra of the graft copolymers from PGMA-co-PMMA while the distinctive methoxy group (*f*) can be observed in (PGMA-co-PSt)-g-PMMA (**5c**). In all cases, the grafting is again associated with a monomodal increase in molecular weight in the GPC profiles.

Two PGMA-co-PMMA compositions (20/80 and 2/98) were synthesized and used in the grafting of St and BA. The 20/80 copolymer provides an average graft density of about one grafted

chain for every ~6 and ~12 main chain repeat units, corresponding to respectively ~80% and ~40% epoxide RRO. The larger amount of epoxide RRO also allows for a slightly narrower molecular weight distribution of the graft copolymer, corresponding to shorter grafted chains. The low epoxide content in the 2/98 copolymer enables the RRO of all epoxide groups. The control of the grafting was also attempted in the absence of CuBr<sub>2</sub> by using an excess of Cp<sub>2</sub>TiCl<sub>2</sub><sup>28–34</sup> (experiments 3–5). Thus, while broad distributions ( $M_w/M_n = 2.3–2.8$ ) are observed at 90 °C, decreasing the temperature to 75 °C and increasing the Ti/epoxide ratio decreases the polydispersity to about 1.4, which is similar to the results obtained in the presence of CuBr<sub>2</sub> and consistent with the temperature and stoichiometry effects on Ti catalyzed styrene polymerizations.<sup>28–34</sup> However, narrower polydispersities are obtained for BA grafting in the presence of CuBr<sub>2</sub> (experiments 6 and 8). PGMA-co-PSt with GMA/St = 46/54 was also used as a macroinitiator for the CuCl<sub>2</sub> assisted graft copolymerization of MMA at 75–90 °C to generate (PGMA-co-PSt)-g-PMMA of two different compositions.

DSC characterization (Figure 5) provides further evidence of grafting. Thus, while  $T_g^{\text{PGMA-co-PMMA (20/80)}} = 95$  °C, at low (<30 mol %) styrene content, a single  $T_g = 107–113$  °C is seen for (PGMA-co-PMMA)-g-PSt. By comparison,  $T_g^{\text{PGMA-co-PMMA (2/98)}} = 106$  °C, and phase separation emerges for PSt > 50 mol %, as evidenced by the bimodality of the transition, with  $T_g^{\text{PGMA-co-PMMA}}$  increasing to about 116 °C and  $T_g^{\text{PSt}} = 97–101$  °C. However, grafting of BA up to 7 mol % does not generate a detectable change in  $T_g^{\text{(PGMA-co-PMMA)-g-PBA}}$  vs  $T_g^{\text{PGMA-co-PMMA (2/98)}}$ . By contrast, while  $T_g^{\text{PGMA-co-PMMA (20/80)}} = 95$  °C, graft copolymers containing 60–90 mol % PBA display a clear transition associated with  $T_g^{\text{PBA}} \sim -45$  °C, while the glass transition of the main chain increases as seen before to  $T_g^{\text{PGMA-co-PMMA}} = 104–108$  °C.

The glass transition of PGMA-co-PSt increases upon PMMA grafting from  $T_g^{\text{PGMA-co-PSt (46/54)}} = 76$  °C to  $T_g^{\text{(PGMA-co-PSt)-g-PMMA}} = 98$  and 108 °C with increasing MMA content from 45% to 68%, respectively. Since PGMA-co-PSt is a random copolymer as demonstrated by NMR,<sup>45</sup> no phase separation is expected in this case.

Table 3.  $\text{Cp}_2\text{TiCl/CuBr}_2$  Catalyzed Sequential Grafting from PGMA

| expt | M   | (macro)initiator                         | M/I/ $\text{Cp}_2\text{TiCl}_2$ /<br>$\text{Zn/CuBr}_2/\text{bpy}^a$ | <i>t</i> (h) | % conv <sup>c</sup> | % RRO <sup>c</sup> | polymer  | comp <sup>c</sup> | $M_n$<br>$M_w/M_n$ | $T_g$<br>(°C) |
|------|-----|--|--|--------------|---------------------|--------------------|--|-------------------|--------------------|---------------|
| 1    | GMA | MBSC                                     | <i>b</i>   | 2            | 94                  | 0                  | PGMA   | 100               | 6400<br>1.12       | 55            |
| 2    | MMA | PGMA                                     | 500/100/5/2.75/<br>5/15  | 4            | 91                  | 16                 | PGMA- <i>g</i> -PMMA                                       | 10/90             | 39868<br>1.41      | 114           |
| 3    | St  | PGMA                                     | 2000/100/5/<br>2.75/5/15   | 23           | 47                  | 17                 | PGMA- <i>g</i> -PSt  | 8/92              | 83000<br>1.57      | 106           |
| 4    | St  | PGMA- <i>g</i> -PMMA                     | 250/(10/90)/0.5/<br>0.25/0.5/1.5                                     | 19           | 16                  | 37                 | (PGMA- <i>g</i> -PMMA)- <i>g</i> -PSt                      | 6/58/36           | 49502<br>1.43      | 92            |
| 5    | MMA | PGMA- <i>g</i> -PSt                      | 176/(8/92)/0.35/<br>0.2/0.3/1  | 24           | 35                  | 38                 | (PGMA- <i>g</i> -PSt)- <i>g</i> -PMMA                      | 5/68/27           | 102967<br>1.48     | 105           |
| 6    | BMA | (PGMA- <i>g</i> -PMMA)-<br><i>g</i> -PSt | 378/(6/58/36)/<br>3.8/3.8/3.8/11.3                                   | 21           | 96                  | 100                | ((PGMA- <i>g</i> -PMMA)- <i>g</i> -PSt)-<br><i>g</i> -PBMA | 1.8/8.6/11.4/68.2 | 132537<br>1.79     | 34<br>106     |
| 7    | BMA | (PGMA- <i>g</i> -PMMA)-<br><i>g</i> -PSt | 756/(6/58/36)/<br>3.8/3.8/3.8/11.3                                   | 42           | 100                 | 100                | ((PGMA- <i>g</i> -PMMA)- <i>g</i> -PSt)-<br><i>g</i> -PBMA | 1/10/6.4/82.6     | 245161<br>2.09     | 36<br>108     |

<sup>a</sup> Molar concentration, all reaction at 90 °C (except expt 1 at 40 °C and expt 3 at 80 °C). <sup>b</sup> GMA/MBSC/CuCl/bpy 50/1/1/3. <sup>c</sup> Determined by <sup>1</sup>H NMR.

**Sequential Grafting.** Once one copolymer is grafted onto PGMA, the remaining unopened epoxide groups can be further used in a sequential grafting manner. Thus, by contrast to other LRP methods which would require additional synthetic steps involving the selective protection/deprotection of the main chain initiator functionality, the Ti/epoxide methodology allows the convenient multiple, sequential, and independent graft copolymerization of a series of different monomers, thus providing easy access to complex polymer architectures.

Several examples are outlined below and summarized in Table 3. The NMR, GPC, and DSC characterizations are shown in Figures 1, 6, and 7. Both PGMA-*g*-PMMA and PGMA-*g*-PSt synthesized as described above still contain about 80% of the original unopened PGMA epoxides, which are available for further grafting. Consequently, a fraction of the remaining epoxides were opened by  $\text{Cp}_2\text{TiCl}$  to a cumulative ~40% RRO vs the original PGMA. The corresponding radicals were used in the initiation of the  $\text{CuBr}_2$ -mediated grafting copolymerization of St and MMA to generate (PGMA-*g*-PMMA)-*g*-PSt and (PGMA-*g*-PSt)-*g*-PMMA, respectively. These miktoarm graft copolymers still contain about 60% of the original epoxides, which can conceivably be used for further initiation. Therefore, all the remaining unopened epoxides of (PGMA-*g*-PMMA)-*g*-PSt were used in the sequential grafting of the third monomer, BMA, to generate ((PGMA-*g*-PMMA)-*g*-PSt)-*g*-PBMA.

The sequential grafting is again demonstrated (Table 3) by the continuous and monomodal molecular weight increase at each iteration. Thus,  $M_n^{\text{PGMA}} = 6400$ ,  $M_n^{\text{PGMA-}g\text{-PMMA}} = 39\,868$ , and  $M_n^{\text{(PGMA-}g\text{-PMMA)-}g\text{-PSt}} = 49\,502$  while  $M_n^{\text{PGMA-}g\text{-PSt}} = 83\,000$ ,  $M_n^{\text{(PGMA-}g\text{-PSt)-}g\text{-PMMA}} = 102\,967$ , and finally  $M_n^{\text{(PGMA-}g\text{-PMMA)-}g\text{-PSt)-}g\text{-PBMA}} = 132\,537$  or 245 161. The NMR spectra (Figure 6) also confirm the presence of the second (St) and third (BMA) sequentially grafted monomers.

The thermal characterization is presented in Figure 7. After the first iteration, the glass transition increases from  $T_g^{\text{PGMA}} = 55$  °C to  $T_g^{\text{PGMA-}g\text{-PMMA (10/90)}} = 114$  °C and  $T_g^{\text{PGMA-}g\text{-PSt (8/92)}} = 106$  °C. Upon the sequential grafting of PSt onto PGMA-*g*-PMMA, phase separation occurs, and consequently, two transitions are observed for (PGMA-*g*-PMMA)-*g*-PSt (6/58/36) at 92 and 115 °C. However, upon sequential grafting of PMMA onto PGMA-*g*-PSt,  $T_g^{\text{(PGMA-}g\text{-PSt)-}g\text{-PMMA (5/68/27)}}$  remains relatively unchanged at 106 °C, most likely due to the overriding effect of the larger St content and the higher molecular weight by comparison with the complementary experiment. A weak transition is also observed at 126 °C and is probably associated with the stiffening of the main chain of PGMA. After the third iteration, upon grafting of PBMA onto

(PGMA-*g*-PMMA)-*g*-PSt, the resulting ((PGMA-*g*-PMMA)-*g*-PSt)-*g*-PBMA displays a lower  $T_g$  associated with PBMA at 34 °C and a higher transition corresponding to the PSt and PMMA chains at 108 °C.

## Conclusion

The first example of the use of epoxides in radical grafting copolymerizations was exemplified by the grafting of PMMA, PBMA, PBA, and PSt from PGMA and from GMA copolymers with MMA and St. A wide range of molecular weights and graft copolymer compositions were synthesized, and the grafting was demonstrated by a combination of GPC, NMR, and DSC investigations.

The polymerization is initiated by the  $\text{Cp}_2\text{TiCl}$ -catalyzed radical ring opening of the epoxide group of GMA and is controlled in the presence of  $\text{CuBr}_2/\text{bpy}$  via reverse ATRP. Epoxides are ubiquitous functional groups in organic and polymer chemistry<sup>47</sup> and are available with a wide variety of structures. In addition, macromolecular epoxides can be obtained from the facile epoxidation of unsaturated polymers (e.g., polyisoprene, etc.), from derivatization with epichlorohydrin, or via copolymerization with GMA. Moreover, while only the Ti/Cu tandem system was studied here, it is likely that both nitroxides and RAFT reagents can be used to control the grafting after the Ti/RRO initiation. Thus, while related architectures could conceivably be obtained using subsequent anionic “grafting onto” polymerizations and coupling sequences, the radical methodology offers the benefit of considerably less stringent reaction conditions and thus more convenient access to complex macromolecular architectures.

A further advantage of this grafting technique was demonstrated by the iterative synthesis of mixed arm graft copolymers such as ((PGMA-*g*-PMMA)-*g*-PSt)-*g*-PBMA. By contrast to other possible synthetic avenues, this method does not require additional epoxide protection/deprotection steps, as the amount of epoxide opening is only controlled by the  $\text{Cp}_2\text{TiCl}$ /epoxide ratio and there is no reaction between Cu halides and epoxides. However, it is possible that the order in which the monomers are sequentially grafted may affect the steric accessibility of remaining epoxides and the distribution of the different grafts along the main chain. These effects as well as the scope and limitations of the sequential procedure are currently under investigation and will be reported soon.

**Acknowledgment.** The National Science Foundation (CHEM-0518247) is gratefully acknowledged for support of this research.

## References and Notes

- Jenkins, D. W.; Hudson, S. M. *Chem. Rev.* **2001**, *101*, 3245–3273.
- Mays, J. W.; Uhrig, D.; Gido, S.; Zhu, Y.; Weidisch, R.; Iatrou, H.; Hadjichristidis, N.; Hong, K.; Beyer, F.; Lach, R.; Buschnakowski, M. *Macromol. Symp.* **2004**, *215*, 111–126.
- Zhang, H.; Ruckenstein, E. *Macromolecules* **1998**, *31*, 4753–4759.
- Hawker, C. J.; Mecerreyes, D.; Elce, E.; Dao, J.; Hedrick, J. L.; Barakat, I.; Dubois, P.; Jerome, R.; Volksen, W. *Macromol. Chem. Phys.* **1997**, *198*, 155–166.
- Hong, S. C.; Pakula, T.; Matyjaszewski, K. *Macromol. Chem. Phys.* **2001**, *202*, 3392–3402.
- Fischer, H. J. *Polym. Sci., Part A: Polym. Chem.* **1999**, *37*, 1885–1901.
- Goto, A.; Fukuda, T. *Prog. Polym. Sci.* **2004**, *29*, 329–385.
- (a) Percec, V.; Barboiu, B. *Macromolecules* **1995**, *28*, 7970–7972. (b) Wang, J. S.; Matyjaszewski, K. *Macromolecules* **1995**, *28*, 7901–7910. (c) Kato, M.; Kamigaito, M.; Sawamoto, M.; Higashimura, T. *Macromolecules* **1995**, *28*, 1721–1723. (d) Kamigaito, M.; Ando, T.; Sawamoto, M. *Chem. Rev.* **2001**, *101*, 3689–3745. (e) Percec, V.; Asandei, A. D.; Asgarzadeh, F.; Bera, K. T.; Barboiu, B. *J. Polym. Sci., Part A: Polym. Chem.* **2000**, *38*, 3839–3843. (f) Percec, V.; Asandei, A. D.; Asgarzadeh, F.; Barboiu, B.; Holerca, M. N.; Grigoras, C. J. *Polym. Sci., Part A: Polym. Chem.* **2000**, *38*, 4353–4361.
- Hawker, C. J.; Bosman, A. W.; Harth, E. *Chem. Rev.* **2001**, *101*, 3661–3688.
- (a) Wayland, B.; Mukerjee, S.; Poszmik, G.; Woska, D.; Basicke, L.; Gridnev, A.; Fryd, M. *ACS Symp. Ser.* **1998**, *685*, 305. (b) Debuigne, A.; Caille, J. R.; Jerome, R. *Angew. Chem., Int. Ed.* **2005**, *44*, 1101–1104. (c) Poli, R. *Angew. Chem., Int. Ed.* **2006**, *45*, 5058–5070.
- Chieffari, J.; Chong, Y. K.; Ercole, F.; Krstina, J.; Jeffery, J.; Le, T. P. T.; Mayadunne, R. T. A.; Meijs, G. F.; Moad, C. L.; Moad, G.; Rizzardo, E.; Thang, S. H. *Macromolecules* **1998**, *31*, 5559–5562.
- (a) Gaynor, S. G.; Wang, J. S.; Matyjaszewski, K. *Macromolecules* **1995**, *28*, 8051–8056. (b) Percec, V.; Popov, A. V.; Ramirez-Castillo, E.; Monteiro, M.; Barboiu, B.; Weichold, O.; Asandei, A. D.; Mitchell, C. M. *J. Am. Chem. Soc.* **2002**, *124*, 4940–4941. (c) Asandei, A. D.; Percec, V. *J. Polym. Sci., Part A: Polym. Chem.* **2001**, *39*, 3392–3418.
- (a) Yamago, S.; Iida, K.; Yoshida, J. *J. Am. Chem. Soc.* **2002**, *124*, 2874–2875. (b) Yamago, S.; Ray, B.; Iida, K.; Yoshida, J.; Tada, T.; Yoshizawa, K.; Kwak, Y.; Goto, A.; Fukuda, T. *J. Am. Chem. Soc.* **2004**, *126*, 13908–13909.
- (a) Matyjaszewski, K.; Xia, J. H. *Chem. Rev.* **2001**, *101*, 2921–2990. (b) Matyjaszewski, K.; Davis, T. P. *Handbook of Radical Polymerization*; Wiley-Interscience: Hoboken, NJ, 2002. (c) Coessens, V.; Pintauer, T.; Matyjaszewski, K. *Prog. Polym. Sci.* **2001**, *26*, 337–377.
- Fischer, H. J. *Polym. Sci., Part A: Polym. Chem.* **1999**, *37*, 1885–1901.
- Handbook of Radical Polymerization*; Matyjaszewski, K., Davis, T. P., Eds.; Wiley-Interscience: New York, 2002; pp 361–462.
- Mahanthappa, M. K.; Waymouth, R. M. *J. Am. Chem. Soc.* **2001**, *123*, 12093–12094.
- (a) Reetz, M. T. In *Organometallics in Synthesis: A Manual*; Schlosser, M., Ed.; John Wiley and Sons: Chichester, England, 2002; pp 817–924. (b) Crabtree, R. H. *The Organometallic Chemistry of the Transition Metals*; John Wiley: New York, 2001. (c) Cardin, D. J.; Lappert, M. F.; Raston, C. L. In *Chemistry of Organo-Zirconium and -Hafnium Compounds*; Wiley and Sons: New York, 1986.
- (a) Gansauer, A.; Rinker, B. *Titanium and Zirconium in Organic Synthesis*; Wiley: New York, 2002. (b) Cuerva, J. M.; Justicia, J.; Oller-López, J. L.; Oltra, J. E. *Top. Curr. Chem.* **2006**, *264*, 63–91.
- Spencer, R. P.; Schwartz, J. *Tetrahedron* **2000**, *56*, 2103–2112.
- (a) Green, M. L. H.; Lucas, C. R. *J. Chem. Soc., Dalton Trans.* **1972**, 1000–1003. (b) Jungst, R.; Sekutowski, D.; Davis, J. Luly, M.; Stucky, J. *Inorg. Chem.* **1977**, *16*, 1645–1655.
- Barden, M. C.; Schwartz, J. *J. Am. Chem. Soc.* **1996**, *118*, 5484–5485.
- Rajanbabu, T. V.; Nugent, W. A. *J. Am. Chem. Soc.* **1994**, *116*, 986–997.
- Ashby, E. C. *Acc. Chem. Res.* **1988**, *21*, 414–421.
- (a) Gansauer, A. *Chem. Commun.* **1997**, 457–458. (b) Yamamoto, Y.; Hattori, R.; Miwa, T.; Nakagai, Y.; Kubota, T.; Yamamoto, C.; Okamoto, Y.; Itoh, K. *J. Org. Chem.* **2001**, *66*, 3865–3870. (c) Enemærke, R. J.; Larsen, J.; Hjøllund, G. H.; Skrydstrup, T.; Daasbjerg, K. *Organometallics* **2005**, *24*, 1252–1262. (d) Enemærke, R. J.; Larsen, J.; Skrydstrup, T.; Daasbjerg, K. *J. Am. Chem. Soc.* **2004**, *126*, 7853–7864.
- Dunlap, M. S.; Nicholas, K. M. *J. Organomet. Chem.* **2001**, *630*, 125–131.
- Barden, M. C.; Schwartz, J. *J. Am. Chem. Soc.* **1996**, *118*, 5484–5485.
- Asandei, A. D.; Moran, I. W. *J. Am. Chem. Soc.* **2004**, *126*, 15932–15933.
- Asandei, A. D.; Chen, Y. *Macromolecules* **2006**, *39*, 7549–7554.
- Asandei, A. D.; Saha, G. J. *Polym. Sci., Part A: Polym. Chem.* **2006**, *44*, 1106–1116.
- (a) Asandei, A. D.; Moran, I. W. *J. Polym. Sci., Part A: Polym. Chem.* **2005**, *43*, 6028–6038. (b) Asandei, A. D.; Moran, I. W. *J. Polym. Sci., Part A: Polym. Chem.* **2005**, *43*, 6039–6047. (c) Asandei, A. D.; Moran, I. W. *J. Polym. Sci., Part A: Polym. Chem.* **2006**, *44*, 1060–1070.
- Asandei, A. D.; Moran, I. W.; Saha, G.; Chen, Y. *J. Polym. Sci., Part A: Polym. Chem.* **2006**, *44*, 2015–2026.
- Asandei, A. D.; Moran, I. W.; Saha, G.; Chen, Y. *J. Polym. Sci., Part A: Polym. Chem.* **2006**, *44*, 2156–2165.
- Asandei, A. D.; Moran, I. W.; Saha, G.; Chen, Y. *ACS Symp. Ser.* **2006**, *944*, 125.
- Asandei, A. D.; Saha, G. *Macromol. Rapid Commun.* **2005**, *26*, 626–631.
- Borner, H. G.; Beers, K.; Matyjaszewski, K.; Sheiko, S. S.; Moller, M. *Macromolecules* **2001**, *34*, 4375–4383.
- (a) Grubbs, R. B.; Dean, J. M.; Bates, F. S. *Macromolecules* **2001**, *34*, 8593–8595. (b) Canamero, P. F.; Fuente, J. L. De.; Madruga, E. L.; Fernandez-Garcia, M. *Macromol. Chem. Phys.* **2004**, *205*, 2221–2228. (c) Krishnan, R.; Srinivasan, K. S. V. *Macromolecules* **2004**, *37*, 3614–3622.
- Yuan, Z.; Gauthier, M. *Macromolecules* **2005**, *38*, 4124–4132.
- (a) Zhang, H.; Ruckenstein, E. *Macromolecules* **1998**, *31*, 4753–4759. (b) Ruckenstein, E.; Zhang, H. *J. Polym. Sci., Part A: Polym. Chem.* **1999**, *37*, 105–112. (c) Zhang, H.; Ruckenstein, E. *Macromolecules* **2000**, *33*, 814–819. (d) Ruckenstein, E.; Zhang, H. *J. Polym. Sci., Part A: Polym. Chem.* **2000**, *38*, 1195–1202.
- Friedrich, J.; Dolg, M.; Gansauer, A.; Geich-Gimbel, D.; Lauterbach, T. *J. Am. Chem. Soc.* **2005**, *127*, 7071–7077.
- Rajanbabu, T. V.; Nugent, W. A. *J. Am. Chem. Soc.* **1989**, *111*, 4525–4527.
- (a) Xia, J.; Matyjaszewski, K. *Macromolecules* **1997**, *30*, 7692–7696. (b) Xia, J.; Matyjaszewski, K. *Macromolecules* **1999**, *32*, 5199–5202.
- Handbook of Chemistry and Physics*, 84th ed.; Lide, D. R., Ed.; CRC Press: Boca Raton, FL, 2004; pp 9–47.
- Paul, S.; Ranby, B. *J. Polym. Sci., Polym. Chem. Ed.* **1976**, *14*, 2449–2461.
- Brar, A. S.; Yadav, A.; Hooda, S. *Eur. Polym. J.* **2002**, *38*, 1683–1690.
- Brandrup, J.; Immergut, E. H.; Grulke, E. A., Eds. *Polymer Handbook*, 4th ed.; Wiley: New York, 1999; p II/226.
- Odian, G. *Principles of Polymerization*, 4th ed.; John Wiley & Sons: New York, 2004; p 128.

MA0618833